

Supplementary Material

Red emissive carbon dots with an ultra-large Stokes shift for multi-channel detections of pesticides

Jing Wang,^a Yaoyao Feng,^{†a} Ping Hu,^a Xiaobo Sun,^a Wei Pan^a and Jinping Wang^{*a}

^a College of Chemical and Pharmaceutical Sciences, Qingdao Agricultural University, Qingdao
266109, PR China.

* Corresponding author. jpwang@qau.edu.cn (Jinping Wang)

† Co-first author

2.1 Materials and apparatus

KCl, NaCl, MgCl₂, CaCl₂, CuCl₂, Fe(NO₃)₃, NH₄Cl, NaNO₃, NaH₂PO₄, Na₂HPO₄, AlCl₃, NaHCO₃, sulfuric acid, HNO₃, phenol, sulfuric acid and m-phenylenediamine were purchased from Damao Chemical Corp (Tianjin, China). Citric acid (CA), ascorbic acid (AA), glutathione (GSH), glutamate (Glu), L-cysteine (Cys), glucose and o-Phenylenediamine (OPD) were obtained from Aladin Ltd (Shanghai, China). All chemicals were used without any further purification. Ultrapure water used throughout all the experiments was purified through Water Purifier Nanopure water system (18.3 MΩ.cm).

The morphology and size of CDs were analyzed using a transmission electron microscopy (TEM, Hitachi H-7700, operated at 80 kV). The X-ray diffraction (XRD) profiles of CDs were collected using a D8 ADVANCE X-ray diffractometer (Bruker AXS, German) with Cu-K α radiation (40 kV, 40 mA, $\lambda = 1.5418 \text{ \AA}$) at a scanning rate of 1° min^{-1} in the range from 10° to 80° . The Fourier transform infrared spectroscopy (FT-IR) spectra were recorded using a FT-IR200 spectrometer (Thermo, America) with KBr pellets technique, over the range $500\text{-}4000 \text{ cm}^{-1}$. UV-vis absorption spectra were scanned by the use of a U-3900 UV-vis spectrophotometer (Hitachi, Japan). The collection of fluorescent spectra was performed by a fluorescence spectrometer F-4600 (Hitachi, Japan).

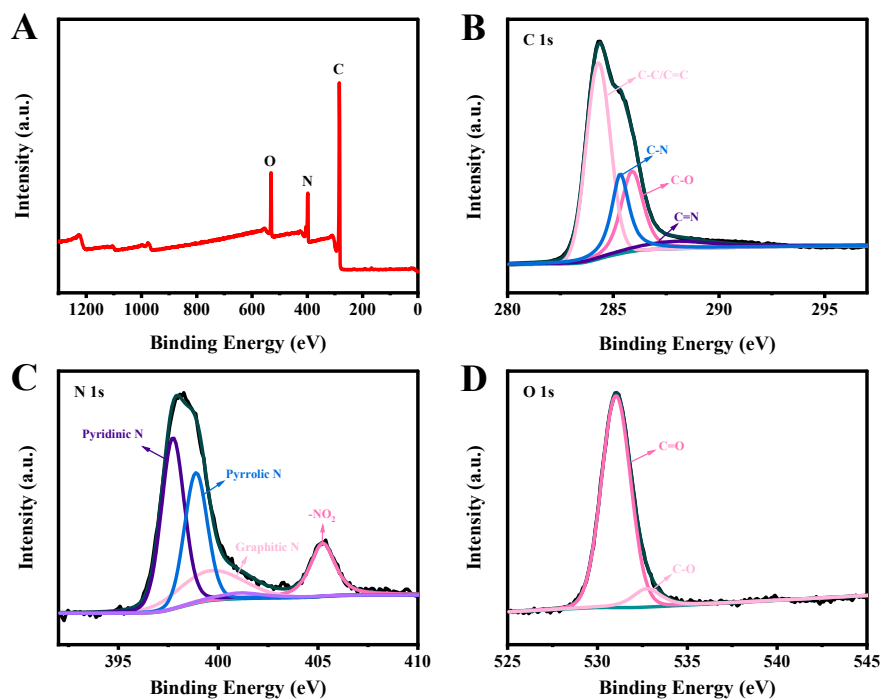


Figure S1. XPS spectra of the R-CDs. (A) the full spectrum; (B) C1s spectrum; (C) N1s spectrum; (D) O1s spectrum.

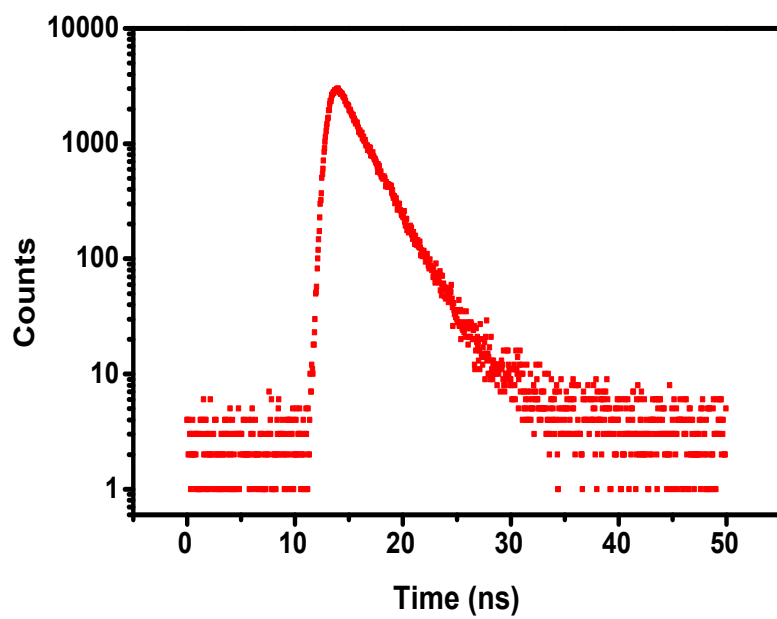


Figure S2. Fluorescence lifetime decay curve of the R-CDs collected at 604 nm.

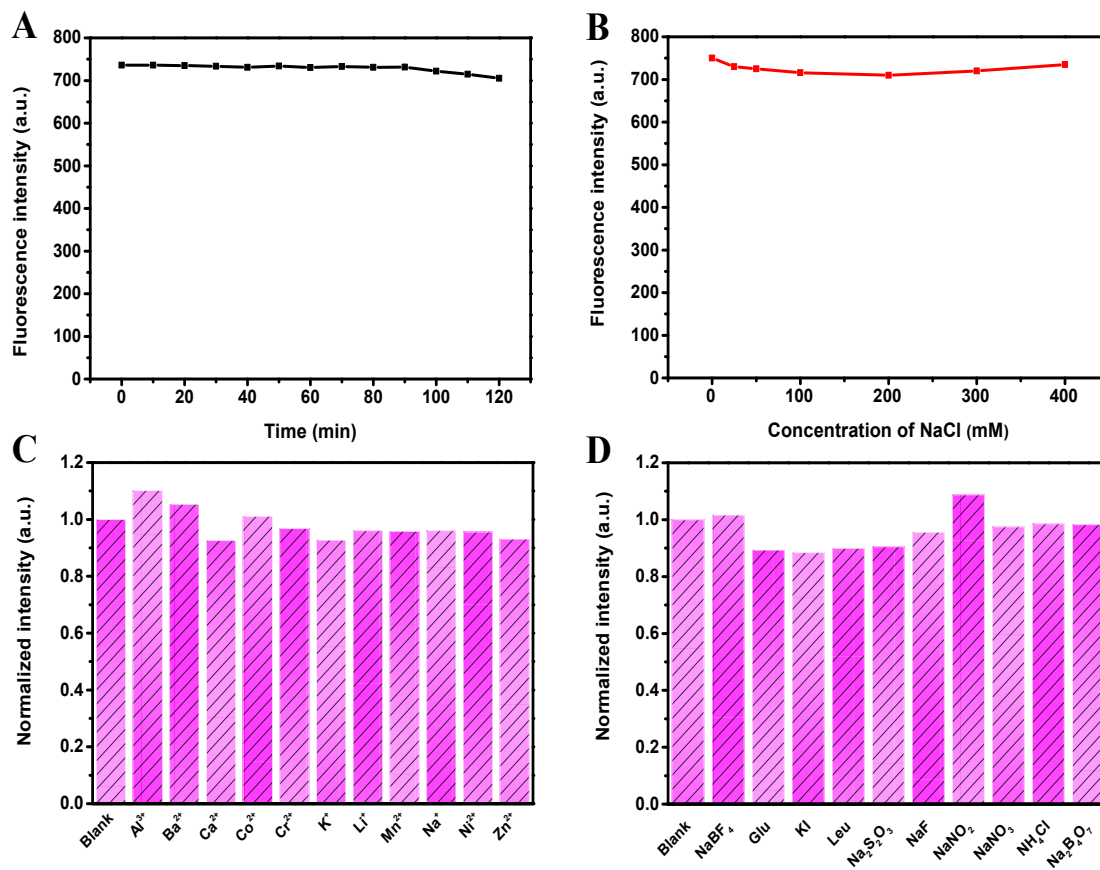


Figure S3. (A) The photostability test of R-CDs in a fluorescence spectrophotometer with a 150 W Xe lamp under excitation at 280 nm (B) The effect of ionic strength on the fluorescence of R-CDs (NaCl solution at the concentration of 0, 25, 50, 100, 200, 400 mM, respectively) (C) The normalized fluorescence intensity of R-CDs in the presence of different metal ions. (D) The normalized fluorescence intensity of R-CDs in the presence of different small molecule substance.

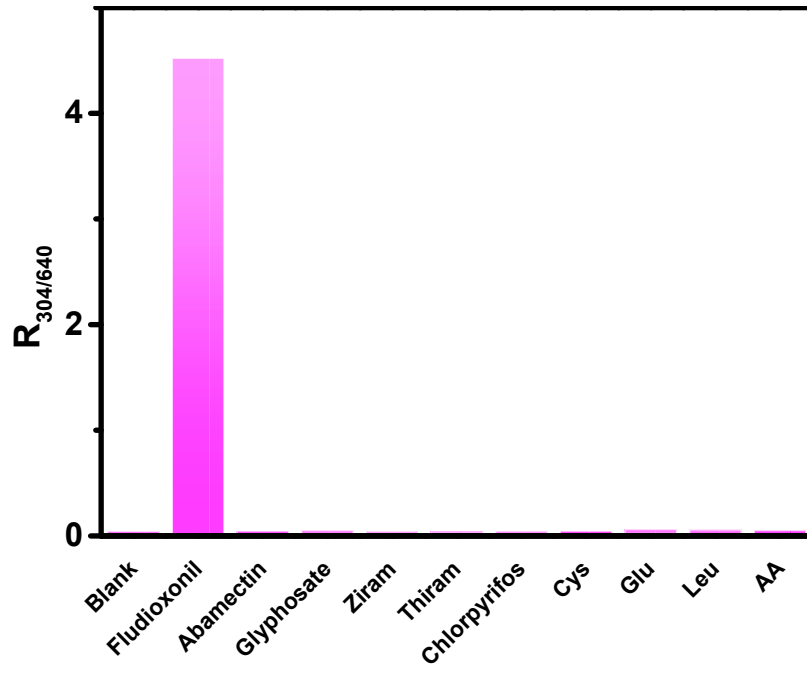


Figure S4. The effects of potential interference substances on $R_{304/640}$. The concentrations of interference substances were 5-fold of fludioxonil.

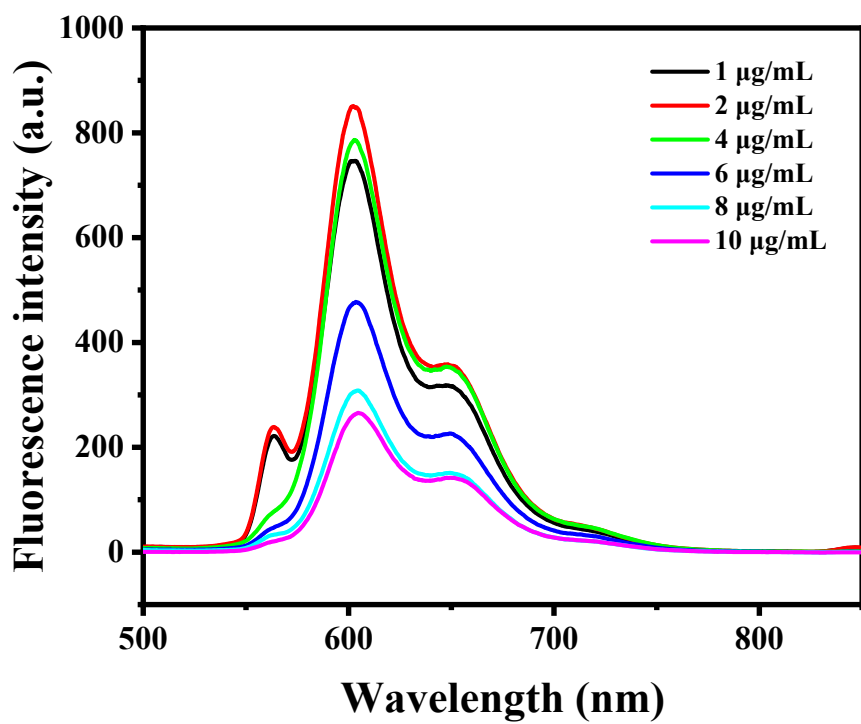


Figure S5. Fluorescence emission spectra of CDs with different concentrations.

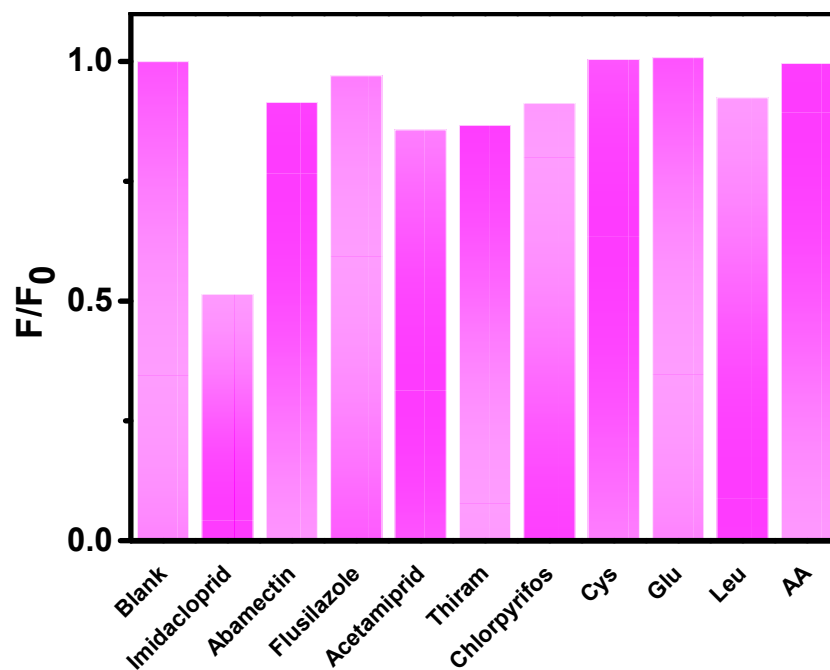


Figure S6. The effects of potential interference substances on the fluorescence intensity of R-CDs.

The concentrations of interfering substances were 5-fold of imidacloprid.

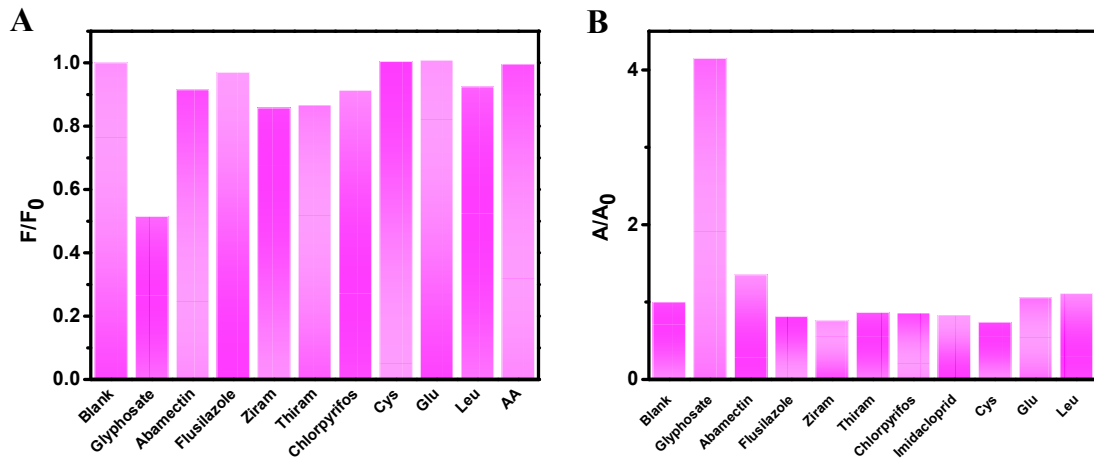


Figure S7. The effects of potential interference substances on the fluorescence intensity of R-CDs and the absorbance. The concentrations of interfering substances were 5-fold of glyphosate.

Table S1. The fluorescence lifetimes of R-CDs at 604 nm with different concentrations of imidacloprid.

Imidacloprid concentration s ($\mu\text{g/mL}$)	τ_1 (ns)	B_1 (%)	τ_2 (ns)	B_2 (%)	τ_{avg} (ns)	χ^2
0	2.3487	96.88	11.0258	3.12	2.61	1.137
1	2.3267	96.07	6.5925	3.93	2.49	1.250
2	2.3056	95.65	5.8948	4.35	2.46	1.210
4	2.4110	100			2.41	1.135
6	2.3568	97.13	10.1787	2.87	2.58	1.185
8	2.3234	96.18	7.0710	3.82	2.50	1.187

Table S2. The fluorescence lifetimes of R-CDs at 604 nm with different concentrations of glyphosate.

Glyphosate concentration s ($\mu\text{g/mL}$)	τ_1 (ns)	B_1 (%)	τ_2 (ns)	B_2 (%)	τ_{avg} (ns)	χ^2
0	2.3325	96.24	6.9946	3.76	2.50	1.178
2	2.1961	95.99	6.3426	4.01	2.36	1.263
4	2.1885	94.15	5.5039	5.85	2.38	1.219
6	2.2021	95.16	6.5937	4.84	2.41	1.112
8	2.2156	94.48	6.2095	5.52	2.43	1.287
10	2.1987	92.32	5.1359	7.68	2.42	1.135

Table S3. Performance comparison of different methods for the determination of fludioxonil, imidacloprid and glyphosate, respectively.

	method	Linear range ($\mu\text{g/mL}$)	LOD ($\mu\text{g/mL}$)	References
Fludioxonil	GC-MS		2.8×10^{-5}	1
	HPLC-UV	0.01-16	0.0042	2
	HPLC	0.035-20	0.03	3
	Fluorometric	0.1-1.0	0.03	This work
	GO/UCNPS	0.08~50ng/mL		4
Imidacloprid	AuNR@Ag	10–400 nM		5
	Tyr-MoO ₃ QDs	0.045–1.00		6
	Fluorescence	1.0	8.23×10^{-4}	7
	Nanoplasmonic platform		0.010	8
	Fluorometric	0.4-6.0	0.10	This work
	Colorometric	50-1000	0.1	9
Glyphosate	Fluorometric	0.025-0.5	0.012	10
	Fluorometric	0.1-16	0.087	11
	DLLME-spectrophotometric	0.5-10	0.21	12
	Fluorimetric		0.009	13
	Fluorometric	1.0-8.0	0.18	
	Colorimetry	1.0-10.0	0.02	This work

Table S4. The results for the detections of fludioxonil, imidacloprid and glyphosate in tap water and pork samples.

Response signal	Sample	Added ($\mu\text{g/mL}$)	Found ($\mu\text{g/mL}$)	Recovery (%)	RSD (%)	
Fludioxonil						
Ratio fluorescence	Tap water	0.00	/	/	/	
		0.30	0.293	97.50	2.58	
		0.50	0.496	99.25	3.09	
		0.70	0.709	101.3	4.28	
	Pork	0.00	/	/	/	
		0.30	0.321	107.00	1.68	
		0.50	0.486	97.25	2.47	
		0.70	0.691	98.67	5.02	
Imidacloprid						
Fluorescence	Tap water	0.00	/	/	/	
		0.50	0.55	110.0	5.32	
		0.90	0.92	102.2	2.65	
		3.00	2.89	96.30	2.34	
	Pork	0.00	/	/	/	
		0.50	0.48	96.00	3.58	
		0.90	0.94	104.10	2.17	
		3.00	3.05	101.60	3.39	
Glyphosate						
Fluorescence	Tap water	0.00	/	/	/	
		3.00	2.96	98.6	4.21	
		5.00	5.12	98.4	3.89	
		7.00	6.89	102.1	4.91	
	Pork	0.00	/	/	/	
		3.00	2.88	96.0	2.21	
		5.00	5.10	102.00	2.09	
		7.00	6.95	99.30	4.85	
	Colorimetric	Tap water	0.00	/	/	/
			3.00	2.93	100.48	6.41
			5.00	5.08	100.77	4.75
			7.00	6.95	98.98	2.61
Pork		0.00	/	/	/	
		3.00	2.97	91.50	5.34	
		5.00	5.10	109.19	6.97	
		7.00	6.90	103.60	3.87	

References

- 1 A. E. Bulgurcuoğlu, B. Y. Durak, D. S. Chormey and S. Bakırdere, *Microchemical Journal*, 2021, **168**, 106381.
- 2 A. Khalid, S. N. Ali, A. Qayoom, S. Iqbal, S. Ansari, Z. u. H. Awan, F. Kishwar and P. Daniel, *Arabian Journal of Chemistry*, 2022, **15**, 103692.
- 3 L. Vaquero-Fernández, A. Sáenz-Hernández, J. Sanz-Asensio, P. Fernández-Zurbano, M. Sainz-Ramírez, B. Pons-Jubera, M. López-Alonso, S.-I. Epifanio-Fernández and M.-T. Martínez-Soria, *Journal of the Science of Food and Agriculture*, 2008, **88**, 1943-1948.
- 4 Y. Guo, R. Zou, F. Si, W. Liang, T. Zhang, Y. Chang, X. Qiao and J. Zhao, *Food Chemistry*, 2021, **335**, 127609.
- 5 Y. Sun, N. Zhang, C. Han, Z. Chen, X. Zhai, Z. Li, K. Zheng, J. Zhu, X. Wang, X. Zou, X. Huang and J. Shi, *Food Chemistry*, 2021, **358**, 129898.
- 6 M. R. Kateshiya, N. I. Malek and S. K. Kailasa, *Journal of Molecular Liquids*, 2020, **319**, 114329.
- 7 J. Luo, S. Li, C. Pang, M. Wang, X. Ma and C. Zhang, *Microchemical Journal*, 2022, **175**, 107172.
- 8 S. H. Wang, S. C. Lo, Y. J. Tung, C. W. Kuo, Y. H. Tai, S. Y. Hsieh, K. L. Lee, S. R. Hsiao, J. F. Sheen, J. C. Hsu and P. K. Wei, *Biosensors & Bioelectronics*, 2020, **170**, 112677.
- 9 H. N. Abdelhamid and H.-F. Wu, *Journal of Materials Chemistry B*, 2013, **1**, 6094.
- 10 H. Li, T. Kang, B. Zhang, J. Zhang and J. Ren, *Computational Materials Science*, 2016, **117**, 33-39.
- 11 J. Hou, X. Wang, S. Lan, C. Zhang, C. Hou, Q. He and D. Huo, *Analytical Methods*, 2020, **12**, 4130-4138.
- 12 E. Cetin, S. Sahan, A. Ulgen and U. Sahin, *Food Chemistry*, 2017, **230**, 567-571.
- 13 J. Jiménez-López, E. J. Llorent-Martínez, P. Ortega-Barrales and A. Ruiz-Medina, *Food Analytical Methods*, 2018, **11**, 1840-1848.